曲げ強度のワイブル分布の分析で希土酸化物系の複合材中の自己治療機能の評価

グエン タン ソン[1]，高橋 剛[1]，中山 忠親[2]
[1]釧路工業高等専門学校　　[2]長岡技術科学大学

Evaluation of self-healing function in rare-earth oxide based-composites by analyzing the Weibull distribution of flexural strength

Son Thanh NGUYEN[1], Tsuyoshi TAKAHASHI[1], Tadachika NAKAYAMA[2]
[1]National Institute of Technology-Kushiro College　　[2]Nagaoka University of Technology

Self-healing is a function that the cracks appear on the surface of a material can be autonomously repaired, and hence helps to recover and in some cases can improve the material's flexural strength. On the other hand, Weibull distribution is widely used for analyzing the strength and predict the fracture probability of a material, therefore can be employed to evaluate its self-healing function. This paper investigates the measured strength of several types of rare-earth oxide-matrix-composites, the candidate materials for the thermal/environmental barrier coatings of the next-gen gas engine turbine blades. Based on the Weibull analysis results, a simple method to determine the appropriate amount of fillers to guarantee the best performance of the self-healing ability is proposed. The results presented here can be good reference data in the process of designing future self-healable ceramic-matrix-composites for high-temperature applications.
Keywords: self-healing, ceramic, composite, Weibull analysis, strength

1. Introduction

The remarkable developing speed of aviation industry has been greatly contributed by the advanced materials. Nickel-based superalloys and thermal barrier coatings (TBCs) are the two important inventions significantly improved the fuel efficiency in gas turbine engine because they helped to increase the engine's inlet temperature.[1,2] To reach higher temperature, in the next generation of air plane engine, the turbine blades would be manufactured from silicon carbide matrix composite,[3] or metallic single crystal superalloys.[4] The light weight, good hardness, and thermal stability at high temperatures of these material promoted they as ideal replacements for the current materials.[5,6] However, both of these candidate materials for turbine blades require to be protected by thermal barrier coatings to endure the very hot gas from combustion chamber. In the case of SiC, the coating is also necessary to avoid the rapid recession of this material in the water vapor environment, therefore it is named as environmental barrier coatings (EBC).[7] Conventionally, TBCs or EBCs are structured with a top coat ceramic layer that have good thermal properties and a bond coat layer to avoid the thermal expansion mismatch between the top coat and the substrate. Ytterbium disilicate ($Yb_2Si_2O_7$) and yttrium titanate ($Y_2Ti_2O_7$) are two of the most promising candidates for the top coat layer because these ceramic have a low thermal conductivity, a coefficient of thermal expansion (CTE) similar to that of SiC or Ni-based superalloy,

and good water corrosion resistance.[7–10] In the case of $Yb_2Si_2O_7$, it also exhibits a stability against the molten calcium-magnesium-alumino-silicate (CMAS), which can be formed from the intake air and harmful to the turbine blades, better than its brother Yb_2SiO_5 (ytterbium monosilicate).[11]

Like many other ceramics, $Yb_2Si_2O_7$ and $Y_2Ti_2O_7$ are brittle materials with low fracture toughness and strength,[12,13] which make them easily cracked caused by foreign debris impact or by residual stress from thermal cycling. The cracks can propagate toward the lower layers of the T/EBCs, leading to the degradation, delamination and spallation of these structures.[14] Therefore, structural ceramics with self-healing ability have been studied to solve this problem.[15–19] At high temperature, this ability is triggered by the oxidation of a healing agent (such as SiC or Ni) dispersed in the ceramic matrix, then the volume expansion of the oxidation products helps to close the cracks. The composites of $Ni/Y_2Ti_2O_7$ or $SiC/Yb_2Si_2O_7$ are considered promising materials for T/EBCs top coat. In previous studies, the authors have been successful in fabricating $Ni/Y_2Ti_2O_7$ composite[20] and $SiC/Yb_2Si_2O_7$ composite[21,22] possessing self-healing ability that can be activated by the surface oxidation at high temperature in air:

$$2Ni + O_2 = 2NiO \quad (I)$$

$$SiC(s) + 2O_2(g) = SiO_2(l) + CO_2(g) \quad (IIa).$$

In these composites, the self-healing ability is triggered from the oxidation of healing agents (Ni or SiC) to form NiO or SiO_2 oxide, whose volume expansion can help to seal the cracks. In the case of $SiC/Yb_2Si_2O_7$ composite, SiO_2 glass in turn reacts with the remaining monosilicate and transformed themselves into the disilicate as follows:

$$SiO_2(l) + Yb_2SiO_5(s) = Yb_2Si_2O_7(s) \quad (IIb).$$

The volume expansion of the newly-formed $Yb_2Si_2O_7$ further contribute to the healing of the surface cracks. A fully healed composite exhibit an enhancement of 20% in bending strength.[]

On the other hand, there have been research on the decomposition of $Yb_2Si_2O_7$ to Yb_2SiO_5 in a water vapor environment,[23,24] raising a concern about the stability of this ceramic as a EBC materials. However, our recent research has confirmed that those decomposed monosilicate can recombine with silica at higher temperature to form disilicate again, and hence further improve the crack healing ability.[25] This result indicates that $SiC/Yb_2Si_2O_7$ can prolong their healing ability for thermal cycling cycles, a critical requirement for the practical application of the material to EBC.

In this paper, we synthesized $SiC/Yb_2Si_2O_7$ composite and $Ni/Y_2Ti_2O_7$ composite by hot-pressing in a gas furnace. The composites were then annealed in air at various temperatures to investigate the self-healing phenomenon of the surface cracks, which were purposely induced by a Vickers indenter. The phase transformation, flexural strength and self-healing mechanisms of the composites were investigated. Then the measured strength values of these rare-earth oxide-matrix-composites were used for Weibull analysis. From the analysis result, the appropriate amount of filler in each kind of composites to guarantee the best performance of the self-healing ability is determined.

2. Materials and Method:

2.1. Fabrication of the composites

First, $SiC/Yb_2Si_2O_7$ composite was synthesized by solid state reaction and hot-pressing method. Yb_2O_3 (99.9%, Shin-Etsu Chemical, Japan) and SiO_2 (99.5%, Sigma Aldrich, USA) powders were first mixed in 1:2 molar ratio, then a corresponding volume fraction (10 vol.%) of cubic SiC nanopowder (IBIDEN, Japan) was added to produce a powder mixture. The mixture was then ball-milled in high purity ethanol overnight, followed by evaporation and drying at 80°C for 24 h. Afterwards, the mixture was dry ball-milled and then sieved to break up agglomerates. Next, this prepared fine

powder mixture was hot-pressed in a sintering furnace (FVPHP-R-5, FRET-18, Fuji Dempa Kogyo, Japan) at 30MPa, 1550°C for 1h, in argon (Ar) gas to obtain sintered disks (44mm in diameter).

The fabrication of $Ni/Y_2Ti_2O_7$ composite was described in a previous work.[26] At first, Y_2O_3 (Shin-Etsu Chemical) and anatase TiO_2 (Sigma Aldrich) was mixed together in 1:2 molar ratio then ball-milled in 99.5% ethanol overnight, followed by dried in an oven at 80°C and calcined at 1200°C in air to obtain $Y_2Ti_2O_7$ fine powder. Then, nickel nitrate $Ni(NO_3)_2{\cdot}6H_2O$ (98%, Wako Pure Chemicals) was mixed with the synthesized $Y_2Ti_2O_7$ powder and the mixture was then ball-milled, dried and grinded before being heated in air furnace at 400°C for 2 h to decompose $Ni(NO_3)_2{\cdot}6H_2O$ and obtain nickel oxide (NiO). Then $NiO/Y_2Ti_2O_7$ mixture powder was subjected to another heat treatment at 800°C for 2 h in a 97% Ar + 3% H_2 environment (gas flowrate=100mL/min). The result of this treatment is a complete reduction of NiO into nickel (Ni). Then $Ni/Y_2Ti_2O_7$ mixture was dry ball-milled to obtain very fine powder for the hot-pressing process. Finally, the synthesized $Ni/Y_2Ti_2O_7$ powder mixture was hot-pressed in an Ar atmosphere at 25MPa and 1340°C for 4h by the above-mentioned furnace to obtain sintered disks (44mm in diameter).

2.2. Measurements and characterizations

For flexural strength measurement, the sintered disks were cut into rectangular specimens (36 mm × 4 mm × 3 mm), then their long edges were beveled at 45°, according to JIS R1601. Flexural strength of the composites was measured at room temperature by four-point bending method using a testing system (MODEL-1311 VRW, Aikoh Engineering, Japan). The outer span L and inner span l were 30 and 10 mm, and the crosshead speed was set at 0.5 mm/min. The bending strength σ_B of a specimen is given by the following equation:

$$\sigma_B = 3P(L - l)/2wt^2 \quad (1)$$

where w and t are the width and thickness of the specimen, and P is the load when the specimen is broken. To investigate the impact of surface cracks on the bending strength, on the surface of specimens, cracks were prepared by using a Vickers hardness tester (HV-100, Mitutoyo, Japan) with 2 kgf indentation load. The as-indented specimens were annealed at 1250°C for 2h ($SiC/Yb_2Si_2O_7$) or 1150°C for 1h ($Ni/Y_2Ti_2O_7$) to activate their crack-healing ability.

The cross-sections of specimens and the indentation cracks were observed using a field-emission scanning electron microscope (JSM-7001FA, JEOL). The identity of healing agents was investigated using an energy-dispersive X-ray spectrometer (EDS) attached to this scanning electron microscope (SEM). The crystalline phases of the synthesized powder mixture and sintered composites were identified using an X-ray diffractometer (XRD, RINT 2500PC, Rigaku, Japan) with Cu-Kα radiation (λ = 1.54186 Å).

2.3. Weibull analysis

The fracture probability P_f as a function of the flexural strength σ_f can be estimated using the following Weibull distribution function:

$$\ln\{\ln(1/(1 - P_f))\} = m\ln(\sigma_f) - m\ln(\sigma_0) \quad (2)$$

where m and σ_0 are Weibull modulus and characteristic strength, respectively. Weibull modulus (or shape parameter) describes the variation in flexural strength. The characteristic strength (or scale parameter) σ_0 represents the strength when the fracture probability is 63.2%. Because m and σ_0 are constants, the left-hand side can be represented as a first-degree-polynomial function of $\ln(\sigma_f)$. If all the values of fracture probability and strength are known, then the scale and shape parameters can be evaluated from the linear regression fitting line. The fracture probability at each value of strength is estimated using the median rank method:

$$P_f = (i - 0.3)/(n + 0.4) \quad (3)$$

where i is the rank of the specimen strength, arranged in ascending order, and n is the number of specimens.

3. Results and Discusion

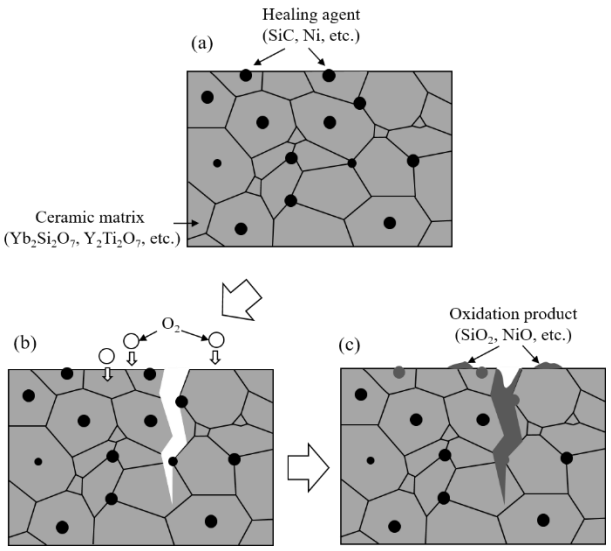

Fig.1. Schematic illustration for surface crack healing: (a) before cracked; (b) after cracked; (c) after healed

Figure 1 illustrates the self-healing phenomenon in these composites. The healing agent particles (SiC or Ni) were dispersed homogeneously in the $Yb_2Si_2O_7$ or $Y_2Ti_2O_7$ ceramic matrix (Fig.1a). The dispersed particles near the composite surface then react with the oxygen in the annealing chamber (Fig.1b) to form oxidation products (grey color), which subsequently seal the cracks on the surface (Fig.1c). Here, the oxide formed from the heating process of healing particles should have volume larger than that of the original particles, to fill in the crack.[27]

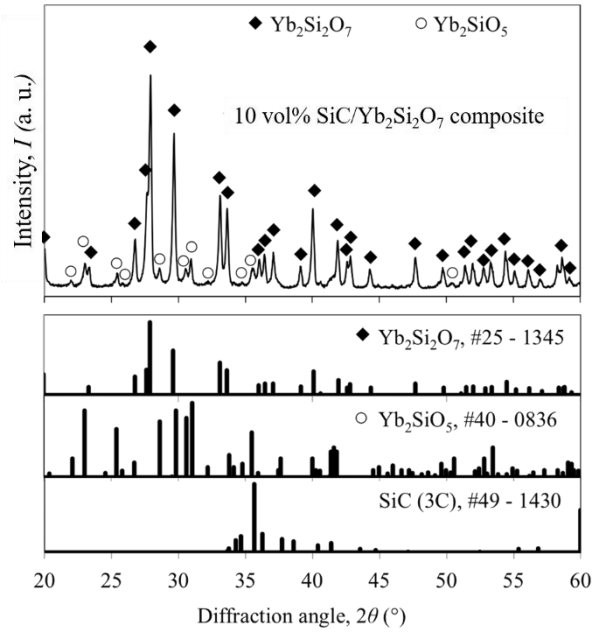

Fig.2 XRD pattern of 10 vol% SiC/$Yb_2Si_2O_7$ composite

Figure 2 shows the XRD pattern of 10 vol% SiC/$Yb_2Si_2O_7$ composite before annealing. The appearance of both $Yb_2Si_2O_7$ and Yb_2SiO_5 diffraction peaks indicates the coexistence of two silicates in the composites, however, the amount of Yb_2SiO_5 is quite small. It is very difficult to identify SiC by this XRD pattern because most of SiC diffraction peaks are overlapped with the silicate peaks. However, the contribution of SiC to the reaction (IIa) and of its oxide (SiO_2) to the reaction (IIb) can be confirmed as follow.

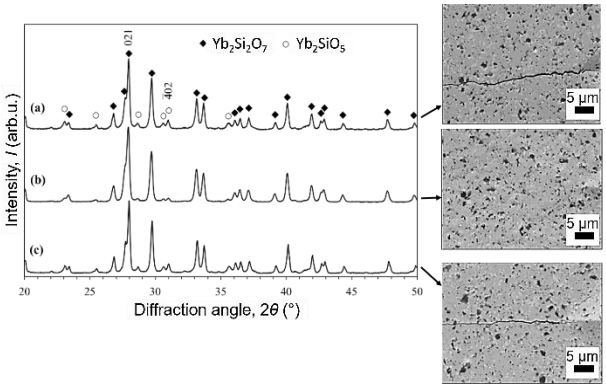

Fig. 3 XRD patterns of 10 vol.% SiC/$Yb_2Si_2O_7$ composite: (a) before annealing; (b) after annealing in air; (c) after annealing in Ar; and their indentation cracks observed by SEM

Figure 3 shows XRD patterns and SEM observation of 10 vol.% SiC/$Yb_2Si_2O_7$ composite, before and after annealing in air or Ar. After annealing in air (b), the diffraction peak intensity of Yb_2SiO_5 became lower, indicating the Yb_2SiO_5 fraction in the composite decreased. In addition, SEM image confirmed that the crack was healed. However, the crack length and XRD peak intensity almost did not change when annealing the composite in Ar (c), indicating that the annealing in inert gas had very limited effect on crack healing. In other words, these results are the evidence for the aforementioned reaction IIa and IIb.

Figure 4 shows the XRD patterns of 10 vol%Ni/$Y_2Ti_2O_7$ composite, before and after the heat treatment at 1150°C for 1 h. The main phase of the fabricated composite is confirmed as $Y_2Ti_2O_7$. In addition, the oxidation of Ni nanoparticles into NiO can be confirmed by this XRD analysis. It is clear

that after the heat treatment, the Ni peaks appeared in upper pattern almost disappeared in the lower pattern. The most recognizable one is the strongest peak of Ni at $2\theta = 44.51°$. On the other hand, several new peaks at $2\theta = 37.06°$, 43.1°, 62.62°, and 79.19° are identified that belong to NiO. The peak at 75.09° is overlapped with the peak at 75.25° of $Y_2Ti_2O_7$ therefore it looks stronger than before the heat treatment.

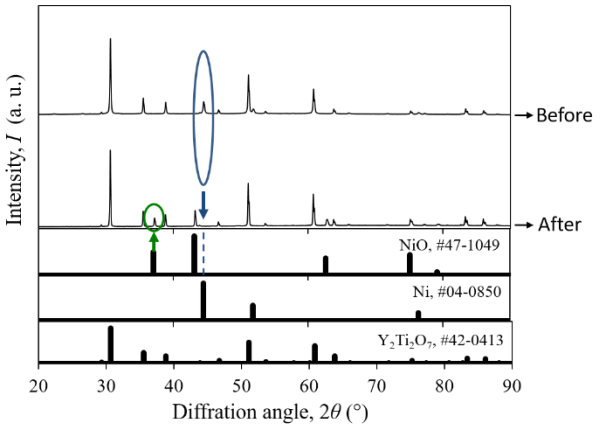

Fig.4. XRD patterns of 10 vol% Ni/$Y_2Ti_2O_7$ composite, before and after the heat treatment

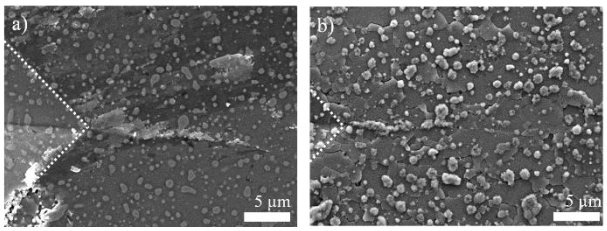

Fig.5. SEM images of a Vickers indentation crack on the surface of 10 vol% SiC/$Yb_2Si_2O_7$ composite, before (a) and after (b) the heat treatment

Figure 5 shows the SEM micrographs of a Vickers indentation on the surface of 10 vol% SiC/$Yb_2Si_2O_7$ composite, before and after the annealing. It can be seen that the crack in Fig.5a almost disappeared after the heat treatment in air (Fig.5b). On the other hand, Figure 6 shows part of a Vickers indentation and its induced crack on the surface of 10 vol% Ni/$Y_2Ti_2O_7$ specimen, before and after the annealing. As can be seen, this crack was also fully healed after the heat-treatment. In this case, the volume expansion can be realized when comparing the size of dispersed particles (Ni) in Fig.6a with their counterparts in Fig.6b (NiO). This confirmed that during the heat-treatment, the healing agent particles were oxidized, expanded, and filled in the cracks.

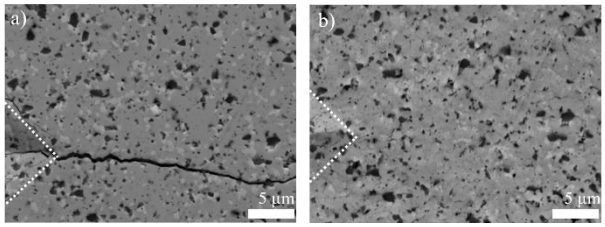

Fig. 6 SEM images of a Vickers indentation crack on the surface of 10 vol% Ni/$Y_2Ti_2O_7$ composite, before (a) and after (b) the heat treatment

The Weibull distribution for the flexural strength of as-sintered, as-indented, and annealed specimens of 10vol% SiC/$Yb_2Si_2O_7$ composite and their fitting lines was shown in Fig.7. The number of samples n was set at 30. The R-squared values in all cases are greater than 95%, indicating good fits. Amongst three groups of specimens, the as-indented has the highest Weibull modulus (m = 10.5), which means they have the narrowest distribution in flexural strength values. The fact that all as-indented specimens are fractured at the Vickers indentation while most of healed specimens have fracture path distant from the indentation (see Fig.8) reveal that indentation cracks are the most severe flaws on the surface of specimens. This explains for a high modulus value of as-indented specimens. However, when the indentation does not exist (as-sintered specimens), a wide distribution of flexural strength can be seen. Weibull modulus in this case decrease to m = 8.2. On the other hand, after the annealing, a higher Weibull modulus (m = 9.8) is obtained. This is because not only the indentation cracks but also all other flaws on the surface were healed. The increase of the Weibull modulus of flexural strength after annealing was also reported in Al_2O_3/SiC self-healing composite.[28]

In addition, the characteristic strength σ_0 at fracture probability of 63.2% for all groups were also calculated and shown. The annealed specimens exhibit a much higher characteristic strength (σ_0 =

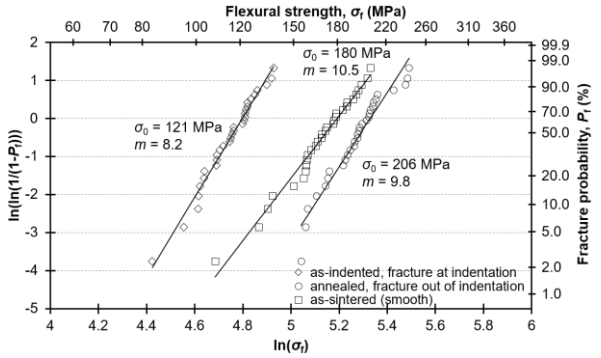

Fig.7. Weibull distribution for flexural strength of 10 vol% SiC/$Yb_2Si_2O_7$ composite

206 MPa) than those of the as-sintered (σ_0 = 180 MPa) and the as-indented (σ_0 = 121 MPa). At the second lowest tensile stress (σ_f = 129 MPa), the fracture probability for the as-indented specimen significantly is high as 88%. In other words, the as-indented specimens are very vulnerable even with very low tensile stress. Meanwhile, at 207 MPa, the highest tensile stress can be attained by an as-sintered specimen, the fracture probability of the annealed specimens is about 70%. This means there is still 30% of probability that the specimens will not be broken. These results prove the significant effect of annealing on improving the fracture resistance of indented specimens.

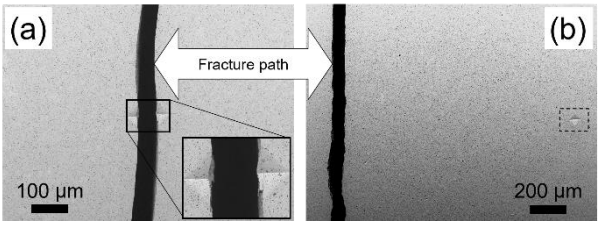

Fig.8. SEM images showing typical fracture paths of (a) as-indented specimen and (b) annealed specimen (notice the Vickers indentations are highlighted in small rectangular)

The Weibull analysis also can be used to predict the maximum volume fraction of healing agent should be introduced to the matrix without causing negative effect. Using the data of $Y_2Ti_2O_7$ flexural strength[29] we plotted a Weibull distribution as shown in Fig.9. and found that the characteristic strength σ_0 = 207 MPa and the Weibull modulus m = 7. From these values, we can calculate the corresponding tensile strength for this material is

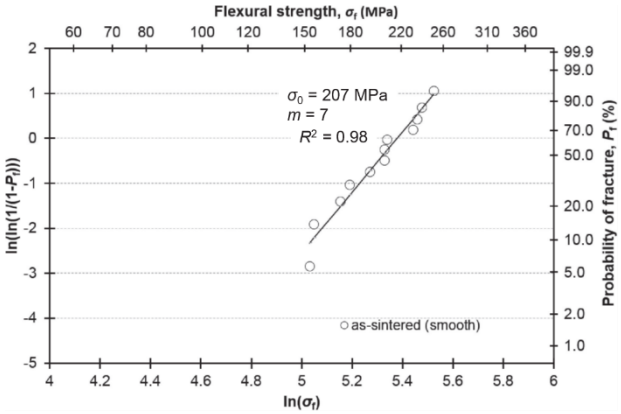

Fig.9. Weibull distribution for flexural strength of $Y_2Ti_2O_7$

σ_t=128 MPa using Munro equation.[30] This value can be considered as the intrinsic strength of $Y_2Ti_2O_7$ ceramic matrix. When the matrix is dispersed with a volume fraction of healing agent (for example: Ni), there would be a thermal mismatch stress between the dispersed particles and the matrix during thermal cycling.[20] The amount of healing agent should be less than a critical value that cause the above stress greater than intrinsic strength. In the case of Ni/$Y_2Ti_2O_7$, the recommended volume fraction of Ni is less than 15 vol%.

4. Summary

In this paper, Ni/$Y_2Ti_2O_7$ and SiC/$Yb_2Si_2O_7$ composites were sintered by a solid state reaction and hot pressing method and their self-healing ability was investigated. The filling up of SiO_2 glass or NiO into the crack and the volume expansion of newly-formed $Yb_2Si_2O_7$ are the key mechanism for the crack healing process. The flexural strength of the composites was also measured and used as the input data to plot the Weibull distribution. From the Weibull analysis, the relationship between fracture behavior and healing effect is elucidated. In addition, it is shown that the maximum amount of healing agent should be introduced to a ceramic matrix can be predicted by this Weibull analysis. The results in this research therefore can be a good reference when designing and characterizing a self-healing ceramic material.

Acknowledgments

The authors are grateful to students at National Institute of Technology-Kushiro College and

Nagaoka University of Technology for their assistance in preparation of specimens and SEM observation. This work was partly supported by Japan Society for the Promotion of Science (JSPS) KAKENHI Grant-in-Aid for Early-Career-Scientists Number 18K14086.

References

[1] J.H. Perepezko, The hotter the engine, the better, Science (80-.). 326 (2009) 1068–1069.

[2] N.P. Padture, Advanced structural ceramics in aerospace propulsion, Nat. Mater. 15 (2016) 804.

[3] I. Spitsberg, J. Steibel, Thermal and Environmental Barrier Coatings for SiC/SiC CMCs in Aircraft Engine Applications, Int. J. Appl. Ceram. Technol. 1 (2004) 291–301.

[4] N.M. Angel, A. Basak, On the Fabrication of Metallic Single Crystal Turbine Blades with a Commentary on Repair via Additive Manufacturing, J. Manuf. Mater. Process. . 4 (2020). https://doi.org/10.3390/jmmp4040101.

[5] F.L. Riley, Structural Ceramics, Cambridge, UK: Cambridge University Press, 2009.

[6] R. Naslain, F. Christin, SiC-Matrix Composite Materials for Advanced Jet Engines, MRS Bull. 28 (2003) 654–658. https://doi.org/10.1557/mrs2003.193.

[7] B.T. Richards, H. Zhao, H.N.G. Wadley, Structure, composition, and defect control during plasma spray deposition of ytterbium silicate coatings, J. Mater. Sci. 50 (2015) 7939–7957. https://doi.org/10.1007/s10853-015-9358-5.

[8] L.R. Turcer, A.R. Krause, H.F. Garces, L. Zhang, N.P. Padture, Environmental-barrier coating ceramics for resistance against attack by molten calcia-magnesia-aluminosilicate (CMAS) glass: Part I, $YAlO_3$ and γ-$Y_2Si_2O_7$, J. Eur. Ceram. Soc. 38 (2018) 3905–3913.

[9] L.R. Turcer, A.R. Krause, H.F. Garces, L. Zhang, N.P. Padture, Environmental-barrier coating ceramics for resistance against attack by molten calcia-magnesia-aluminosilicate (CMAS) glass: Part I, YAlO3 and γ-Y2Si2O7, J. Eur. Ceram. Soc. (2018). https://doi.org/10.1016/j.jeurceramsoc.2018.03.021.

[10] H. Klemm, Silicon nitride for high-temperature applications, J. Am. Ceram. Soc. 93 (2010) 1501–1522.

[11] F. Stolzenburg, M.T. Johnson, K.N. Lee, N.S. Jacobson, K.T. Faber, The interaction of calcium–magnesium–aluminosilicate with ytterbium silicate environmental barrier materials, Surf. Coatings Technol. 284 (2015) 44–50.

[12] N. Al Nasiri, N. Patra, D. Horlait, D.D. Jayaseelan, W.E. Lee, Thermal Properties of Rare-Earth Monosilicates for EBC on Si-Based Ceramic Composites, J. Am. Ceram. Soc. 99 (2016). https://doi.org/10.1111/jace.13982.

[13] W. Song, S. Yang, M. Fukumoto, Y. Lavallée, S. Lokachari, H. Guo, Y. You, D.B. Dingwell, Impact interaction of in-flight high-energy molten volcanic ash droplets with jet engines, Acta Mater. (2019). https://doi.org/10.1016/j.actamat.2019.04.011.

[14] B.T. Richards, S. Sehr, F. de Franqueville, M.R. Begley, H.N.G. Wadley, Fracture mechanisms of ytterbium monosilicate environmental barrier coatings during cyclic thermal exposure, Acta Mater. 103 (2016) 448–460. https://doi.org/10.1016/j.actamat.2015.10.019.

[15] M. Li, C. Huang, B. Zhao, H. Liu, J. Wang, Z. Liu, Crack-healing behavior of Al2O3-TiB2-TiSi2 ceramic material, Ceram. Int. (2018). https://doi.org/10.1016/j.ceramint.2017.10.164.

[16] K. Houjou, K. Ando, K. Takahashi, Crack-healing behaviour of ZrO2/SiC composite ceramics, Int. J. Struct. Integr. 1 (2010) 73–84.

[17] M.D. Hager, P. Greil, C. Leyens, S. van der Zwaag, U.S. Schubert, Self-healing materials, Adv. Mater. 22 (2010) 5424–5430.

[18] W.N. and S. Abe, W. Nakao, S. Abe, W.N. and S. Abe, Enhancement of the self-healing ability in oxidation induced self-healing ceramic by modifying the healing agent, Smart Mater. Struct. 21 (2012) 25002.

[19] T. Osada, K. Kamoda, M. Mitome, T. Hara, T. Abe, Y. Tamagawa, W. Nakao, T. Ohmura, A Novel Design Approach for Self-Crack-Healing Structural Ceramics with 3D Networks of Healing Activator, Sci. Rep. 7 (2017).

[20] S.T. Nguyen, T. Nakayama, M. Takeda, N.N. Hieu, T. Takahashi, Development of Yttrium Titanate/Nickel Nanocomposites with Self Crack-Healing Ability and Potential Application as Thermal Barrier Coating Material, Mater. Trans. (2020). https://doi.org/10.2320/matertrans.MT-MN2019006.

[21] S.T. Nguyen, T. Nakayama, H. Suematsu, T. Suzuki, L. He, H. Cho, K. Niihara, Strength improvement and purification of $Yb_2Si_2O_7$-SiC nanocomposites by surface oxidation treatment, J. Am. Ceram. Soc. 100 (2017) 3122–3131.

[22] S.T. Nguyen, T. Nakayama, H. Suematsu, H. Iwasawa, T. Suzuki, K. Niihara, Self-crack healing ability and strength recovery in ytterbium disilicate/silicon carbide nanocomposites, Int. J. Appl. Ceram. Technol. 16 (2019) 39–49. https://doi.org/10.1111/ijac.13089.

[23] S. Ueno, T. Ohji, H.T. Lin, Recession behavior of $Yb_2Si_2O_7$ phase under high speed steam jet at high temperatures, Corros. Sci. (2008). https://doi.org/10.1016/j.corsci.2007.06.014.

[24] E. Bakan, Y.J. Sohn, W. Kunz, H. Klemm, R. Vaßen, Effect of processing on high-velocity water vapor recession behavior of Yb-silicate environmental barrier coatings, J. Eur. Ceram. Soc. 39 (2019) 1507–1513.

[25] S.T. Nguyen, T. Nakayama, T. Takahashi, H. Suematsu, D.T.M. Do, A. Okawa, K. Niihara, Recycling of a Healing Agent by a Water-Vapor Treatment to Enhance the Self-Repair Ability of Ytterbium Silicate-Based Nanocomposite in Multiple Crack-Healing Test, Adv. Eng. Mater. (2020) 2000157.

[26] S.T. Nguyen, T. Nakayama, H. Suematsu, T. Suzuki, M. Takeda, K. Niihara, Low thermal conductivity $Y_2Ti_2O_7$ as a candidate material for thermal/environmental barrier coatings, Ceram. Int. 42 (2016) 11314-11323. https://doi.org/10.1016/j.ceramint.2016.04.052.

[27] L. Boatemaa, C. Kwakernaak, S. van der Zwaag, W.G. Sloof, Selection of healing agents for autonomous healing of alumina at high temperatures, J. Eur. Ceram. Soc. 36 (2016) 4141–4145. https://doi.org/10.1016/j.jeurceramsoc.2016.05.038.

[28] T. Osada, W. Nakao, K. Takahashi, K. Ando, S. Saito, Strength recovery behavior of machined Al_2O_3/SiC nano-composite ceramics by crack-healing, J. Eur. Ceram. Soc. 27 (2007) 3261–3267.

[29] S.T. Nguyen, T. Nakayama, H. Suematsu, T. Suzuki, M. Nanko, H.-B. Cho, M.T.T. Huynh, W. Jiang, K. Niihara, Synthesis of molten-metal corrosion resistant yttria-based refractory by hot-pressing and densification, J. Eur. Ceram. Soc. 35 (2015) 2651-2662. https://doi.org/10.1016/j.jeurceramsoc.2015.02.023.

[30] M. Munro, Evaluated material properties for a sintered alpha-alumina, J. Am. Ceram. Soc. 80 (1997) 1919–1928.